

Multifunctional Superconducting Nanowire Quantum Sensors

Benjamin J. Lawrie,^{1,*} Claire E. Marvinney,^{1,†} Yun-Yi Pai,¹ Matthew A. Feldman,¹ Jie Zhang,¹ Aaron J. Miller,² Chengyun Hua,¹ Eugene Dumitrescu,³ and Gábor B. Halász¹

¹*Materials Science and Technology Division, Oak Ridge National Laboratory, 1 Bethel Valley Rd, Oak Ridge, TN 37831*

²*Quantum Opus LLC, 22241 Roethel Dr Ste A, Novi, MI 48375*

³*Computational Science and Engineering Division, Oak Ridge National Laboratory, 1 Bethel Valley Rd, Oak Ridge, TN 37831*

(Dated: March 19, 2021)

Superconducting nanowire single photon detectors (SNSPDs) offer high-quantum-efficiency and low-dark-count-rate single photon detection. In a growing number of cases, large magnetic fields are being incorporated into quantum microscopes, nanophotonic devices, and sensors for nuclear and high-energy physics that rely on SNSPDs, but superconducting devices generally operate poorly in large magnetic fields. Here, we demonstrate robust performance of amorphous SNSPDs in magnetic fields of up to ± 6 T with a negligible dark count rate and unchanged quantum efficiency at typical bias currents. Critically, we also show that in the electrothermal oscillation regime, the SNSPD can be used as a magnetometer with sensitivity of better than $100 \mu\text{T}/\sqrt{\text{Hz}}$ and as a thermometer with sensitivity of $20 \mu\text{K}/\sqrt{\text{Hz}}$ at 1 K. Thus, a single photon detector integrated into a quantum device can be used as a multifunctional quantum sensor capable of describing the temperature and magnetic field on-chip simply by varying the bias current to change the operating modality from single photon detection to thermometry or magnetometry.

Superconducting nanowire single photon detectors (SNSPDs) offer high speed, high quantum-efficiency, and low dark-count-rate single photon detection [1]. There is an emerging need for SNSPDs capable of operating in large magnetic fields for potential integration with quantum nanophotonic circuits [2–4] and for quantum sensors relevant to nuclear physics [5] and dark matter detection [6–8]. In general, SNSPDs do not perform well in large magnetic fields, but some research has demonstrated that small magnetic fields can improve SNSPD performance as described below.

SNSPDs can detect photons when (a) the photon provides enough energy to break an ensemble of Cooper pairs and generate a bath of quasiparticles that form a belt across the width of the nanowire, (b) the photon provides enough energy to unpin a vortex, enabling it to sweep across the nanowire under a Lorentz force, and (c) the photon provides enough energy to form and unbind a vortex-antivortex pair that are swept in opposite directions across the nanowire under a Lorentz force. Field-dependent studies of bright count rates have suggested that vortex motion is the primary detection mechanism in typical NbN SNSPDs [9, 10]. Similar measurements

of $\text{Mo}_x\text{Si}_{1-x}$ SNSPDs with varying wire width have concluded that vortex-antivortex interactions are responsible for bright counts in wide devices made from micron-scale wires while direct quasiparticle belt formation is responsible for bright counts in nanowires of order 100 nm in width [11]. A growing body of literature has made it clear that SNSPDs constructed of different materials with different designs can rely on any of the bright-count mechanisms described above [12].

Dark counts are observed as a result of thermally induced vortex motion in the absence of any photons, and are generally present even in well shielded detectors operated at 0 T [13, 14]. Because the local vortex pinning potential can be a spatially heterogeneous function of the superconducting film growth conditions and the device geometry, dark counts may arise preferentially from weak spots within the device. Early models suggested that the energy barrier for single vortex crossing is lower than that for phase slips and vortex-antivortex nucleation and annihilation [13] and that vortex-antivortex interactions and phase slips may be ignored, but competing models and measurements have suggested that vortex-antivortex interactions resulting from a Berezinskii-Kosterlitz-Thouless transition are responsible for SNSPD dark counts [15–17].

At high bias currents, hotspots periodically form and disappear with frequency determined by the device inductance and load impedance, leading to detection of dark counts at this electrothermal oscillation frequency [18–22]. The propagation velocity of a normal-superconducting boundary in the nanowire due to Joule heating depends on its critical current [19], which itself has a strong dependence on the applied external magnetic field. While detection events in the electrothermal oscillation regime are a result of a fundamentally different physical process than dark counts detected at lower bias

* lawriej@ornl.gov; This manuscript has been authored by UT-Battelle, LLC, under contract DE-AC05-00OR22725 with the US Department of Energy (DOE). The US government retains and the publisher, by accepting the article for publication, acknowledges that the US government retains a nonexclusive, paid-up, irrevocable, worldwide license to publish or reproduce the published form of this manuscript, or allow others to do so, for US government purposes. DOE will provide public access to these results of federally sponsored research in accordance with the DOE Public Access Plan (<http://energy.gov/downloads/doe-public-access-plan>).

† marvinneyce@ornl.gov

currents, we describe both conventional dark counts and electrothermal oscillations as dark counts in this article for linguistic convenience.

Current crowding at sharp bends can result in a reduced potential barrier for vortex motion and an increased vortex nucleation density. However, external magnetic fields and associated Meissner currents can reduce the effect of current crowding [23, 24]. Early modeling efforts suggested that perpendicular magnetic fields would reduce the critical current for a conventional meander line SNSPD, but small negative perpendicular magnetic fields could increase the critical current of devices patterned in a spiral layout [23]. Other experimental efforts found a slight asymmetry in the dark count rate of TaN and NbN SNSPDs as a function of field [25, 26], consistent with previous modeling [23], subject to the assumption that dark counts originate largely at the sharp corners of the device and allowing for some heterogeneity in the device fabrication [25].

Understanding and controlling vortex motion and hotspot formation in SNSPDs is critical to the development of quantum sensors capable of operating in high magnetic fields, but fully predictive models of single-photon interactions with superconducting nanowires remain a challenge, despite the recent demonstration of a probabilistic criterion for single photon detection based on single vortex motion [27]. Very little work has explored the field dependence of SNSPDs in large magnetic fields, though one recent article did demonstrate that NbN nanowire single photon detectors can be operated in fields as high as 5 T [28], and many researchers have explored the response of superconducting thin films and nanowires in larger magnetic fields [29–34]. Further research is needed to provide an improved understanding of vortex motion in superconducting nanowires and to define the limits of high-field SNSPD operation.

Here, we explore the magnetic field dependence of dark counts and bright counts generated by a commercially available amorphous transition-metal silicide near-infrared SNSPD with a critical temperature of 5 K. In order to minimize the density of vortices generated by the magnetic field, we focus on magnetic fields oriented parallel to the device. The 7 nm thick SNSPD used here has a 70 nm wide meander line with a 50 percent fill fraction that spans an $11 \times 11 \mu\text{m}$ active area (Quantum Opus, LLC). It was mounted on a PCB and suspended in a dilution refrigerator with free-space optical access to the mixing chamber at an angle of $< 5^\circ$ from a magnetic field that was swept from -6 to 6 T. The SNSPD meander line pattern was oriented at an angle of $\sim 45^\circ$ relative to the field. Unless otherwise specified, the SNSPD temperature was held at 100 mK. An attenuated 1062 nm CW laser source was delivered to the SNSPD through a free-space optical interface with the dilution refrigerator that is described elsewhere [35]. Dark counts were collected with optical access to the dilution refrigerator blocked. All signals were passed through a low frequency filter mounted directly to the SNSPD at the mixing chamber in

order to minimize latching and enable high count rate detection [36]. The bias current and the SNSPD waveforms were delivered along the same semirigid coaxial channel with a room temperature bias tee and low noise amplifiers integrated before time tagging all detection events with a 62 mV threshold. Data was collected (1) continuously for counts as a function of magnetic field for a constant bias current and (2) in 1 T increments for counts as a function of bias current.

The magnetic field dependence of the measured counts is shown as a function of bias current in Fig. 1. At each point on the curve, the bright count rate was averaged for 20 seconds and the dark count rate was averaged for 10 seconds. At all field values, the relative quantum efficiency of the device remains unchanged at bias currents within the quantum efficiency plateau between 7.5-9.5 μA . Additionally, the dark count rate was measured to be < 0.1 counts per second within the same 7.5-9.5 μA range for all measured fields. However, as emphasized in the inset of Fig. 1, the maximum operating bias current is suppressed in an asymmetric manner with increasing field, with positive parallel magnetic fields reducing the maximum operational bias current to $\sim 10.0 \mu\text{A}$ at 6 T, while the maximum operational bias current at -6 T is only reduced to $\sim 11.5 \mu\text{A}$. A similar, if less pronounced asymmetry is present in the onset of bright count detection events at bias currents of 4-5.5 μA as seen in Fig. 1.

This asymmetric magnetic field response leads to a decrease in the dark count rate of the device at some negative fields, and thus an improved operation of the

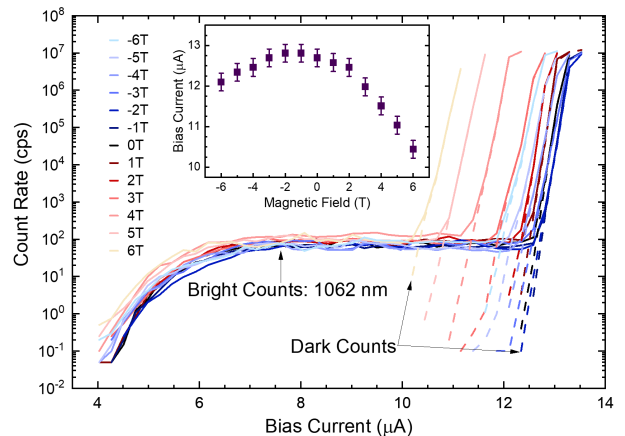


FIG. 1: Measured count rate as a function of bias current and magnetic field for bias currents of 0-14 μA and magnetic fields of -6 to 6 T oriented roughly parallel to the film and $\sim 45^\circ$ to the length of the nanowires. Dark counts begin to contaminate the bright count measurements at bias currents above 10.0 μA . Inset of the bias current at which the dark counts are equal to 10x the plateau bright counts, emphasizing the asymmetry of the field dependence of dark counts at high bias currents.

device between 0 T and -2.5 T, as shown in Fig. 2. This asymmetry was repeatable for multiple zero-field recoiling measurements. The transport properties of the high-count-rate board were also tested separately as a function of field, resulting in no evidence of asymmetry. Thus the asymmetric response shown in Fig. 2 appears to be due to the SNSPD itself. While slight asymmetries in the field-dependent SNSPD response have been reported before for mT-scale perpendicular fields and ascribed to magnetic-field induced currents that oppose current crowding effects at the corners of the meander line [23, 25, 26], the asymmetries reported here rely on similar bias currents but magnetic fields three orders of magnitude larger. Thus, the previous models for asymmetric SNSPD responses to magnetic fields do not appear to explain this result. Notably, while the onset of bright counts and dark counts is a function of magnetic field, and while the SNSPD waveform can be a function of the photon-nanowire interaction parameters [22, 37], the SNSPD waveforms recorded here were independent of field.

While a detailed model of this field-reversal asymmetry is beyond the scope of this article, we can understand why the asymmetry is much larger than in previous works by recognizing the different orientation of the magnetic field and considering the symmetries of the meander line and the bias current. The amorphous superconductor is deposited onto a 120 nm SiO₂ backreflector and the meander line is then capped with a 1.5 nm conformal Al₂O₃ coating to prevent oxidation before 100 nm SiO₂ and Si₃N₄ antireflective coating layers are deposited. If the top and bottom interfaces of the SNSPD are not identical, as is the case here, a field with a finite component along the long line segments is expected to have a field-reversal asymmetry. Indeed, based on the model in Ref. [23], such a field should, depending on its sign, induce current crowding close to the top or the bottom interface, thus giving different rates for positive

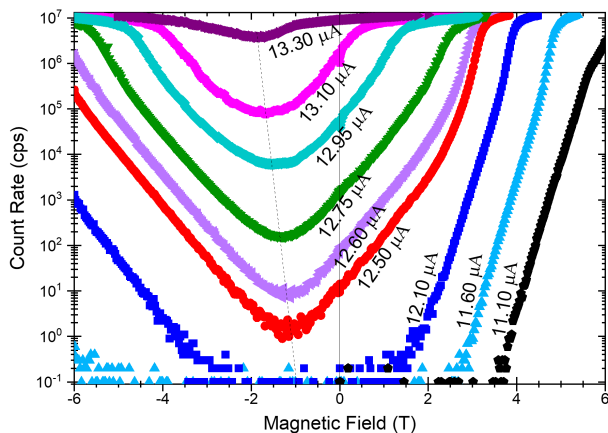


FIG. 2: Dark count rate as a function of field for bias currents of 11.10-13.30 μA .

and negative fields. Moreover, even if the two interfaces are identical, a field-reversal asymmetry is expected if all three components of the field (parallel to the long line segments, the short line segments, and the perpendicular direction, respectively) are finite. In contrast, such a field-reversal asymmetry is forbidden for a purely perpendicular field, regardless of whether the top and bottom interfaces are identical or distinct. For a perpendicular field, it can then only appear due to imperfections of the meander line [25] and is expected to be much smaller.

The magnetic-field dependence of the dark counts in the high-bias-current regime is intriguing because it suggests that the SNSPD can be utilized as an on-chip magnetometer. For a well characterized SNSPD, monitoring changes in the dark count rate after initially setting the bias current to achieve dark counts of $\sim 10^2 - 10^6 \text{ cps}$ provides magnetic field sensitivity determined by the slope of the curves shown in Figs 2 and 3 and limited by the uncertainty in counting statistics and bias current. Here, we assume that the field sensitivity can be calculated based on exponential fits to the measured dark counts and that the measured dark counts exhibit Poissonian counting statistics with uncertainty in count rate scaling as \sqrt{N} . Uncertainty in the bias current is neglected as a small component relative to the uncertainty in count rate. Further, uncertainty in photon counting is a fundamental limit that cannot be improved upon for this type of measurement, whereas the uncertainty in bias current can be improved beyond current limits with further engineering.

The maximum sensitivity of the curves shown in Fig. 2 ranges from $1.8 \text{ mT}/\sqrt{\text{Hz}}$ for a bias current of $13.3 \mu\text{A}$ at -1 T to $600 \mu\text{T}/\sqrt{\text{Hz}}$ for a bias current of $11.10 \mu\text{A}$ at 6T, with the best sensitivity at smaller bias currents closer to the onset of the electrothermal oscillation regime. The best sensitivity measured here was $75 \mu\text{T}/\sqrt{\text{Hz}}$ for a bias current of $11.60 \mu\text{A}$ at 4.8 T. Thus, the SNSPD can be used as a magnetometer by sweeping the bias current while monitoring the dark count rate to coarsely determine the magnetic field and by monitoring changes in the dark count rate at a constant bias current to track smaller changes in the magnetic field.

Extrapolating the results shown in Fig. 1 to larger fields suggests that a plateau with optimized quantum efficiency and minimized dark counts should still exist for fields as large as 18 T and -68 T. It is likely that this extrapolation overestimates the robustness of the SNSPD, as the SNSPD operation relies in part on the description of the SNSPD as a 2D superconductor. For fields above 6.5 T, the characteristic length scale $\sqrt{\hbar/2eB}$ is smaller than the 7 nm film thickness, and that description fails [30]. Nonetheless, it is clear from the results in Fig. 1 that the SNSPD is capable of robust operation for fields much larger than 6 T.

At higher temperatures, the maximum functional bias current is reduced as thermally induced vortex motion begins to increase, but the same robust high quantum-efficiency, low dark-count-rate operation is observed at all

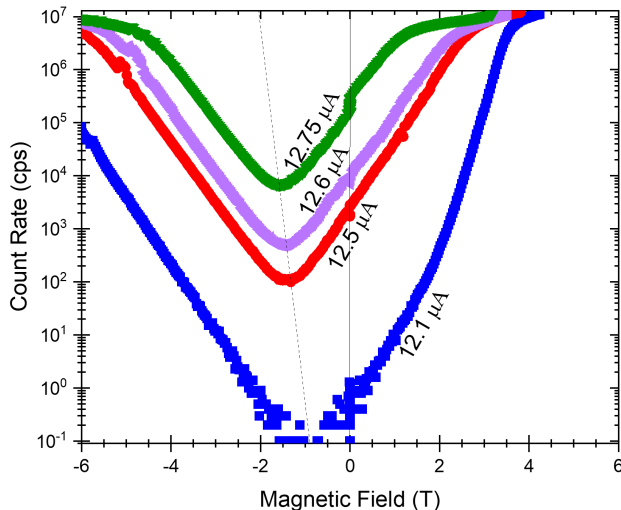


FIG. 3: Dark count rate as a function of field for bias currents of 12.10-12.75 μA at ~ 600 mK.

measured fields for bias currents of 6-12.1 μA . As seen in Fig. 3 for dark counts measured at ~ 600 mK, a similar asymmetry is present in the dark count rate, with the minimum dark counts measured for fields between -1 T and -2 T.

Because this SNSPD was mounted to a PCB at a distance of several inches from the nearest thermometer, there is some uncertainty in the SNSPD temperature that would normally be challenging to quantify. However, the dark counts can be used for thermometry just as they can be used for magnetometry. Figure 4 illustrates the measured dark counts for 12.60 μA and 12.75 μA bias currents at 0 T. As above, the sensitivity of this superconducting nanowire thermometer can be calculated by curve fitting the dark count rate and assuming that the uncertainty in the count rate is limited by the photon counting statistics. The data shown in Fig. 4a illustrate temperature sensitivity of $20 \mu\text{K}/\sqrt{\text{Hz}}$ at a temperature of 1 K and a bias of 12.75 μA , and a temperature sensitivity of $45 \mu\text{K}/\sqrt{\text{Hz}}$ for a 12.60 μA current. At 800 mK, the sensitivity is reduced to $0.1 \text{ mK}/\sqrt{\text{Hz}}$ and $1.5 \text{ mK}/\sqrt{\text{Hz}}$, and at 400 mK, the sensitivity is reduced to $6 \text{ mK}/\sqrt{\text{Hz}}$ and $40 \text{ mK}/\sqrt{\text{Hz}}$, respectively at the larger and smaller bias currents. However, further increasing the bias current does continue to increase the sensitivity, and the SNSPD thermometer is most sensitive when the device is operating in the electrothermal oscillation regime with greater than 10^6 dark counts per second. With the device operating at a higher bias current, this regime can be reached at lower temperatures, and the onset of the electrothermal oscillations near 100 mK will improve the temperature sensitivity. For example, on the cusp of the electrothermal oscillating regime at 60 mK, the sensitivity is improved to better than $0.5 \text{ mK}/\sqrt{\text{Hz}}$, as shown with a bias current of 12.95 μA in Fig. 4b. This

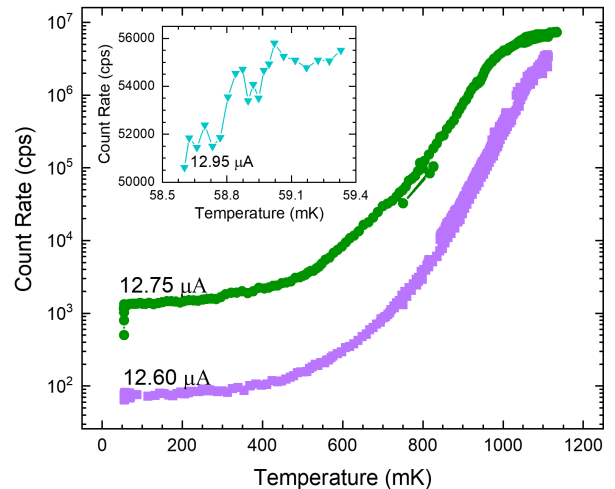


FIG. 4: Temperature dependent dark counts for 12.60 μA and 12.75 μA bias currents at 0 T. The inset illustrates the temperature sensitivity at lower temperatures for a 12.95 μA bias current at 0T.

improved sensitivity comes at the expense of increasing the device temperature ~ 5 mK at a bias current of 14 μA .

The ability to use the SNSPD in large magnetic fields for thermometry or magnetometry in addition to single photon detection is of interest, not just to better quantify the SNSPD operating conditions, but to provide a multifunctional sensor in integrated quantum nanophotonic devices. While the results described in this article provide a device-level understanding of the limitations of thermometry and magnetometry with SNSPDs in large fields, a microscopic understanding of the quasi-particle and vortex interactions that drive this functionality is still needed. Confocal optical microscopies capable of monitoring the SNSPD response as a function of the position and wavelength of incident photons at milliKelvin temperatures and in variable magnetic fields would provide an improved understanding of these interactions at the mesoscale. Additionally, a quantitative model of the magnetic field dependent and temperature dependent electrothermal oscillation frequencies will be pursued as a future work. MilliKelvin scanning probe microscopies including scanning SQUID microscopies [38] and scanning single photon microscopies [35] could help to provide further understanding of these interactions.

ACKNOWLEDGMENTS

This research was sponsored by the U. S. Department of Energy, Office of Science, Basic Energy Sciences, Materials Sciences and Engineering Division. Postdoctoral (CEM) research support was provided by the Intelligence Community Postdoctoral Research Fellowship Program at the Oak Ridge National Laboratory, administered by

Oak Ridge Institute for Science and Education through an interagency agreement between the U.S. Department of Energy and the Office of the Director of National Intelligence. Student (MAF, BEL) research support were

provided by the Department of Defense through the National Defense Science & Engineering Graduate Fellowship (NDSEG) and by the DOE Science Undergraduate Laboratory Internships (SULI) program.

-
- [1] C. M. Natarajan, M. G. Tanner, and R. H. Hadfield, Superconducting nanowire single-photon detectors: physics and applications, *Superconductor science and technology* **25**, 063001 (2012).
- [2] S. Khasminskaya, F. Pyatkov, K. Slowik, S. Ferrari, O. Kahl, V. Kovalyuk, P. Rath, A. Vetter, F. Henrich, M. M. Kappes, *et al.*, Fully integrated quantum photonic circuit with an electrically driven light source, *Nature Photonics* **10**, 727 (2016).
- [3] C. E. Dreyer, A. Alkauskas, J. L. Lyons, A. Janotti, and C. G. Van de Walle, First-principles calculations of point defects for quantum technologies, *Annual Review of Materials Research* **48**, 1 (2018).
- [4] P. Rath, O. Kahl, S. Ferrari, F. Sproll, G. Lewes-Malandrakis, D. Brink, K. Ilin, M. Siegel, C. Nebel, and W. Pernice, Superconducting single-photon detectors integrated with diamond nanophotonic circuits, *Light: Science & Applications* **4**, e338 (2015).
- [5] H. Azzouz, S. N. Dorenbos, D. De Vries, E. B. Ureña, and V. Zwiller, Efficient single particle detection with a superconducting nanowire, *AIP Advances* **2**, 032124 (2012).
- [6] K. K. Berggren, Snowmass2021-letter of interest dark matter detection using layered materials and superconducting nanowires, *SnowMass* (2021).
- [7] J. A. JPL, J. Chiles, B. K. JPL, A. Lita, J. Luskin, S. W. Nam, M. S. JPL, V. Verma, and E. W. JPL, Snowmass2021-letter of interest superconducting nanowire single-photon detectors, *SnowMass* (2021).
- [8] Y. Hochberg, I. Charaev, S.-W. Nam, V. Verma, M. Colangelo, and K. K. Berggren, Detecting sub-gev dark matter with superconducting nanowires, *Physical review letters* **123**, 151802 (2019).
- [9] D. Y. Vodolazov, Y. P. Korneeva, A. Semenov, A. Korneev, and G. Goltsman, Vortex-assisted mechanism of photon counting in a superconducting nanowire single-photon detector revealed by external magnetic field, *Physical Review B* **92**, 104503 (2015).
- [10] R. Lusche, A. Semenov, Y. Korneeva, A. Trifonov, A. Korneev, G. Gol'Tsman, and H.-W. Hübers, Effect of magnetic field on the photon detection in thin superconducting meander structures, *Physical Review B* **89**, 104513 (2014).
- [11] Y. P. Korneeva, N. Manova, I. Florya, M. Y. Mikhailov, O. Dobrovolskiy, A. Korneev, and D. Y. Vodolazov, Different single-photon response of wide and narrow superconducting mx si $1-x$ strips, *Physical Review Applied* **13**, 024011 (2020).
- [12] A. Engel, J. Lonsky, X. Zhang, and A. Schilling, Detection mechanism in snspd: numerical results of a conceptually simple, yet powerful detection model, *IEEE Transactions on Applied Superconductivity* **25**, 1 (2014).
- [13] L. Bulaevskii, M. Graf, C. Batista, and V. Kogan, Vortex-induced dissipation in narrow current-biased thin-film superconducting strips, *Physical Review B* **83**, 144526 (2011).
- [14] L. N. Bulaevskii, M. J. Graf, and V. G. Kogan, Vortex-assisted photon counts and their magnetic field dependence in single-photon superconducting detectors, *Physical Review B* **85**, 014505 (2012).
- [15] T. Yamashita, S. Miki, K. Makise, W. Qiu, H. Terai, M. Fujiwara, M. Sasaki, and Z. Wang, Origin of intrinsic dark count in superconducting nanowire single-photon detectors, *Applied Physics Letters* **99**, 161105 (2011).
- [16] A. Engel, A. Semenov, H.-W. Hübers, K. Il'in, and M. Siegel, Fluctuation effects in superconducting nanostrips, *Physica C: Superconductivity and its applications* **444**, 12 (2006).
- [17] J. Kitaygorsky, I. Komissarov, A. Jukna, D. Pan, O. Minaeva, N. Kaurova, A. Divochiy, A. Korneev, M. Tarkhov, B. Voronov, *et al.*, Dark counts in nanostructured nbn superconducting single-photon detectors and bridges, *IEEE Transactions on Applied Superconductivity* **17**, 275 (2007).
- [18] R. Hadfield, A. J. Miller, S. W. Nam, R. L. Kautz, and R. E. Schwall, Low-frequency phase locking in high-inductance superconducting nanowires, *Applied Physics Letters* **87**, 203505 (2005).
- [19] A. J. Kerman, J. K. Yang, R. J. Molnar, E. A. Dauler, and K. K. Berggren, Electrothermal feedback in superconducting nanowire single-photon detectors, *Physical review B* **79**, 100509 (2009).
- [20] D. Liu, L. You, S. Chen, X. Yang, Z. Wang, Y. Wang, X. Xie, and M. Jiang, Electrical characteristics of superconducting nanowire single photon detector, *IEEE transactions on applied superconductivity* **23**, 2200804 (2013).
- [21] K. K. Berggren, Q.-Y. Zhao, N. Abebe, M. Chen, P. Ravindran, A. McCaughan, and J. C. Bardin, A superconducting nanowire can be modeled by using spice, *Superconductor Science and Technology* **31**, 055010 (2018).
- [22] C. E. Marvinney, B. E. Lerner, A. A. Puretzky, A. J. Miller, and B. J. Lawrie, Waveform analysis of a large-area superconducting nanowire single photon detector, *Superconductor Science and Technology* **34**, 035020 (2021).
- [23] J. R. Clem, Y. Mawatari, G. Berdiyrov, and F. Peeters, Predicted field-dependent increase of critical currents in asymmetric superconducting nanocircuits, *Physical Review B* **85**, 144511 (2012).
- [24] K. Ilin and M. Siegel, Magnetic field stimulated enhancement of the barrier for vortex penetration in bended bridges of thin tan films, *Physica C: Superconductivity and its Applications* **503**, 58 (2014).
- [25] A. Engel, A. Schilling, K. Il'in, and M. Siegel, Dependence of count rate on magnetic field in superconducting thin-film tan single-photon detectors, *Physical Review B* **86**, 140506 (2012).
- [26] I. Charaev, A. Semenov, K. Ilin, and M. Siegel, Magnetic-field enhancement of performance of superconducting nanowire single-photon detector, *IEEE Transactions on*

- Applied Superconductivity **29**, 1 (2019).
- [27] S. Jahani, L.-P. Yang, A. Buganza Tepole, J. C. Bardin, H. X. Tang, and Z. Jacob, Probabilistic vortex crossing criterion for superconducting nanowire single-photon detectors, *Journal of Applied Physics* **127**, 143101 (2020).
- [28] T. Polakovic, W. Armstrong, V. Yefremenko, J. Pearson, K. Hafidi, G. Karapetrov, Z.-E. Meziani, and V. Novosad, Superconducting nanowires as high-rate photon detectors in strong magnetic fields, *Nuclear Instruments and Methods in Physics Research Section A: Accelerators, Spectrometers, Detectors and Associated Equipment* **959**, 163543 (2020).
- [29] H. J. Gardner, A. Kumar, L. Yu, P. Xiong, M. P. Warsawithana, L. Wang, O. Vafek, and D. G. Schlom, Enhancement of superconductivity by a parallel magnetic field in two-dimensional superconductors, *Nature physics* **7**, 895 (2011).
- [30] R. Rosenbaum, Superconducting fluctuations and magnetoconductance measurements of thin films in parallel magnetic fields, *Phys. Rev. B* **32**, 2190 (1985).
- [31] V. Rouco, C. Navau, N. Del-Valle, D. Massarotti, G. P. Papari, D. Stornaiuolo, X. Obradors, T. Puig, F. Tafuri, A. Sanchez, *et al.*, Depairing current at high magnetic fields in vortex-free high-temperature superconducting nanowires, *Nano letters* **19**, 4174 (2019).
- [32] R. Córdoba, T. Baturina, J. Sesé, A. Y. Mironov, J. De Teresa, M. Ibarra, D. Nasimov, A. Gutakovskii, A. Latyshev, I. Guillamón, *et al.*, Magnetic field-induced dissipation-free state in superconducting nanostructures, *Nature communications* **4**, 1 (2013).
- [33] N. Samkharadze, A. Bruno, P. Scarlino, G. Zheng, D. DiVincenzo, L. DiCarlo, and L. Vandersypen, High-kinetic-inductance superconducting nanowire resonators for circuit qed in a magnetic field, *Physical Review Applied* **5**, 044004 (2016).
- [34] X. Zhang, A. Engel, Q. Wang, A. Schilling, A. Semenov, M. Sidorova, H.-W. Hübers, I. Charaev, K. Ilin, and M. Siegel, Characteristics of superconducting tungsten silicide $wxsi_{1-x}$ for single photon detection, *Physical Review B* **94**, 174509 (2016).
- [35] B. Lawrie, M. Feldman, C. Marvinney, and Y. Pai, Free-space confocal magneto-optical spectroscopies at millikelvin temperatures, arXiv preprint arXiv:2103.06851 (2021).
- [36] A. Miller and T. Rambo, Noise suppressing interface circuit for device with control circuits in different noise environments (2020), US Patent App. 16/399,207.
- [37] C. Cahall, K. L. Nicolich, N. T. Islam, G. P. Lafyatis, A. J. Miller, D. J. Gauthier, and J. Kim, Multi-photon detection using a conventional superconducting nanowire single-photon detector, *Optica* **4**, 1534 (2017).
- [38] L. Ceccarelli, D. Vasyukov, M. Wyss, G. Romagnoli, N. Rossi, L. Moser, and M. Poggio, Imaging pinning and expulsion of individual superconducting vortices in amorphous $mosi$ thin films, *Physical Review B* **100**, 104504 (2019).